



ELSEVIER

Nuclear Instruments and Methods in Physics Research B 171 (2000) 2–16

NIM B
Beam Interactions
with Materials & Atoms

www.elsevier.nl/locate/nimb

Atomic and molecular physics using positron accumulation techniques – Summary and a look to the future

C.M. Surko ^{a,*}, R.G. Greaves ^b, K. Iwata ^{a,1}, S.J. Gilbert ^a^a *Physics Department, University of California, San Diego, La Jolla, CA 92093, USA*^b *First Point Scientific, Inc., 5330 Derry Ave., Suite J, Agoura Hills, CA, USA*

Received 18 November 1999; received in revised form 2 February 2000

Abstract

An overview is presented of current techniques to accumulate and cool large numbers of positrons from a radioactive ²²Na source and neon moderator, and the first operation of a new generation of positron accumulator is described. Experiments are discussed that use these techniques to study the interaction of positrons with atoms and molecules at low energies (i.e., below the threshold for positronium formation), including systematic studies of the dependence of positron annihilation on chemical composition. By measuring the Doppler-broadening of gamma-ray annihilation radiation, the quantum state of the annihilating electrons in atoms and molecules was identified. These experiments indicate that positrons annihilate with approximately equal probability on any valence electron. Annihilation with inner shell electrons is infrequent, but is measurable at the level of a few percent in heavier atoms. Measurements of annihilation rates in molecules as a function of positron temperature revealed a number of interesting trends that are briefly discussed. We have developed a new technique to make a cold, bright positron beam. This technique is now being used for a new generation of scattering experiments in the range of energies ≤ 1 eV. Other possible experiments to study aspects of atomic and molecular physics using positron accumulation techniques and this cold positron beam are briefly discussed. © 2000 Elsevier Science B.V. All rights reserved.

PACS: 34.50.-s; 78.70.Bj; 71.60.+z; 36.10.-k*Keywords:* Positrons; Annihilation; Atomic physics; Molecular physics

1. Introduction

While many facets of the interaction of positrons with atoms and molecules are understood [1–9], a number of important questions remain which have potential impact on fields such as atomic physics and gamma-ray astronomy, and technological uses of positrons such as mass spectroscopy and characterizations of solid surfaces. For

* Corresponding author. Tel.: +1-858-534-6880; fax: +1-858-534-0173.

E-mail address: csurko@ucsd.edu (C.M. Surko).

¹ Current address: Physics Research Laboratory, University of California, San Francisco, 389 Oyster Point Blvd., Suite #1, South San Francisco, CA 94080, USA.

example, one problem of current interest is understanding the process of low-energy positron annihilation in large molecules [10]. As another example, experiments are just beginning to study the excitation of molecular vibrations using positrons [11].

We have developed a Penning–Malmberg trap to accumulate positrons efficiently, using a buffer gas to trap the particles [12–14]. This technique has provided new opportunities to study the interaction of positrons with matter at low energies (i.e., at energies below the threshold for positronium atom formation). In the vacuum environment of the accumulator, the two-body interaction of positrons with atoms and molecules can be studied with precision. This has proven to be particularly useful for weak processes, such as annihilation below the threshold for positronium formation, where maximizing the signal-to-noise ratio is an important consideration. The trapped positrons can be confined for long times in the accumulator in order to maximize the interaction with the test species. Using this method, annihilation studies have now been conducted for a wide range of atoms and molecules [4,8,9].

One quantity of interest is the annihilation rate, which is a unique and sensitive measure of short-range correlation between the positron and the bound electrons. Historically, annihilation rates for small atoms and molecules have been expressed in terms of the parameter Z_{eff} , which is the annihilation rate relative to that for positrons in a gas of uncorrelated electrons (i.e., the Dirac annihilation rate). It is defined by

$$\Gamma = \pi r_0^2 c n_m Z_{\text{eff}}, \quad (1)$$

where Γ is the annihilation rate, r_0 the classical electron radius, c the speed of light, and n_m the number density of atoms or molecules. For large molecules, it has been observed that Z_{eff} can exceed the total number of electrons in the molecule, Z , by many orders of magnitude [12,15,16]. In this case, Z_{eff} is simply a normalized annihilation rate, and it bears no relation to the number of electrons in the molecule. While the physical process responsible for these high annihilation rates is not fully understood, these large rates have been in-

terpreted as evidence of the existence of some kind of long-lived positron-molecule states. For electrons and positrons in opposite spin states, positron annihilation in the presence of atomic-density electrons occurs by emission of two 511 keV photons in a time $\sim 10^{-10}$ s. Therefore, depending on the value of Z_{eff} , interaction times can range from about the elastic collision time $\sim 10^{-15}$ – 10^{-10} s [8], and the longer interaction times will result in correspondingly larger values of Z_{eff} .

In order to explore further the nature of positron interaction with atoms and molecules, a technique was developed to measure the Doppler-broadening of the 511 keV annihilation gamma-ray line [4,9]. These measurements provide information about the momentum distributions of the annihilating electron–positron pairs, and hence information about the momentum distributions of the bound electrons. In the positron accumulator it is possible to achieve good statistics, even for small atoms, in acquisition times of a few hours. For room-temperature positrons interacting with neutral matter, the line-broadening is dominated by the momenta of the bound electrons, and so the gamma-ray signal provides information about the electronic states participating in the annihilation process. Using this technique, we have been able to identify the specific annihilation sites (i.e., electronic states) in atoms and molecules.

To study interactions as a function of positron energy, we developed a technique to heat the trapped positrons. This technique is useful for energies up to 0.2 eV for molecules (at which point excitation of molecular vibrations begins to be an excessive heat sink) and up to 0.5 eV in noble gas atoms [17]. To complement the positron heating technique, we have recently been able to create a cold positron beam with an energy resolution less than 20 meV FWHM, tunable from 0.1 eV upwards, and this should permit study of positron interactions as a function of energy with excellent resolution up to hundreds of eV. The first use of this cold positron beam for scattering from atoms and molecules [11] is reviewed in a separate paper in this volume by Gilbert et al. [18].

In the following sections, an overview is presented of progress in accumulator and cold beam technology for use in studying low-energy positron

interactions with atoms and molecules. The present state of experiments to study annihilation on these species is reviewed, with emphasis on the high values of Z_{eff} observed in molecules. The relationship of these data to theories of annihilation in molecules and possibilities for future experiments in this area are discussed. The present state of this subject of annihilation in molecules, including a discussion of open questions is summarized in greater detail in a recent paper by Iwata et al. [10]. Related discussions of theory and numerical calculations can be found in the work of Gribakin and da Silva [19,20].

2. Overview of experimental techniques

The experiments are conducted in a specially designed positron accumulator that has been described in detail previously [5,12,13,21]. This design is based on the Penning–Malmberg trap, which was developed to achieve long-time confinement of electron plasmas [22]. Positrons from a radioactive ^{22}Na source are first slowed to a few eV using a neon rare-gas moderator. There is an ap-

plied magnetic field of $\sim 0.1\text{--}0.15$ T in the z direction. The positrons are injected into the accumulator at energies ~ 30 eV, and inelastic collisions with N_2 molecules are used to trap the positrons. The accumulator has three ‘stages’, which we denote as I, II and III, each with successively lower gas pressure and electrostatic potential. Following a series of inelastic collisions, the positrons are trapped in stage III, where the pressure is $< 1 \times 10^{-6}$ Torr. The positrons cool to room temperature in ~ 1 s, and the positron lifetime in the third stage is ≥ 40 s, limited by annihilation on the N_2 gas. Using this technique, we are able to accumulate $> 10^8 e^+$ in a few minutes from a 90 mCi ^{22}Na source. The lifetime of these positron plasmas with the buffer gas removed ranges from tens of minutes to hours, depending upon the quality of the vacuum.

2.1. New positron accumulator

The design of the original positron accumulator (circa 1985) is shown in the upper part of Fig. 1. This design used two separate magnets with a pumping port between them in order to achieve

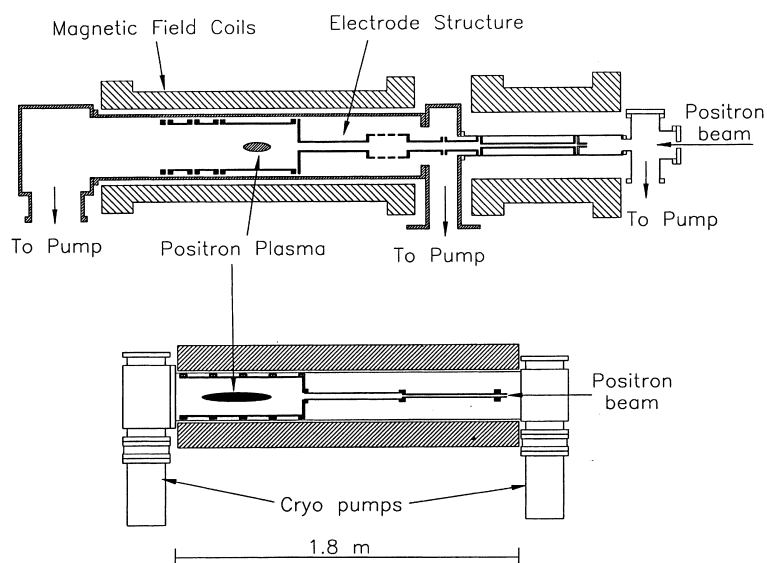


Fig. 1. Shown to scale are the designs of the original (above) and the new positron accumulator (below). The new design is more compact and less expensive to construct and provides true UHV-quality vacuum and the ability to easily modify the electrode structure.

the required differential pumping. Recently, we completed the construction of a new accumulator which eliminates the separate pumping port for the second stage. The new electrode structure was designed using a state-of-the-art molecular flow simulation program, provided by Dr. Tim Bartel of Sandia National Laboratory [23]. The calculated pressure profile along the magnetic axis permits a pressure drop from 1×10^{-3} Torr in stage I to $\leq 2 \times 10^{-8}$ Torr in stage III in a distance of ~ 1 m. The accumulator efficiency is maximized at a somewhat smaller pressure differential, and so it spans more than the range of pressures of interest. The new design is a significant improvement in terms of the pressure uniformity in stage II. In addition, the size of the electrodes and magnet were reduced, thereby reducing complexity and cost. The new vessel is an ultra-high vacuum (UHV) system, bakeable to 130°C , with a base pressure of $\leq 1 \times 10^{-10}$ Torr.

Shown in Fig. 2 is the positron filling as a function of time under conditions in which the trap is operated to maximize the number of positrons trapped. The depth of the potential well was lowered from 10 to 15 V during filling, since at these plasma densities, the trapped positrons create an appreciable space charge. The maximum number of positrons trapped is just under 3×10^8 .

A UHV environment is helpful for many applications. We have been able to accomplish this in the new buffer-gas trap by rapidly pumping out the gas after the positron fill cycle. As shown in Fig. 3, we are able to cycle stage III from an operating

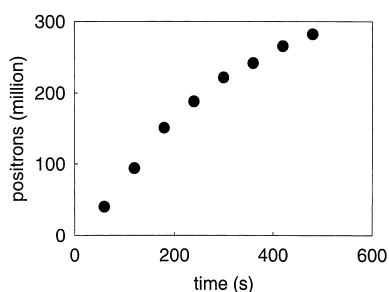


Fig. 2. Positron filling in the new accumulator for a stage-III pressure of 3×10^{-7} Torr. The depth of the potential well was increased from 10 to 15 V during the fill to compensate for the space charge of the positron plasma.

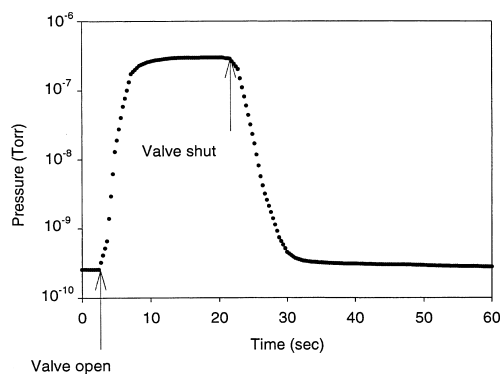


Fig. 3. Pressure in stage III of the new accumulator can be decreased by three orders of magnitude in 10 seconds, providing rapid access to UHV.

pressure of 3×10^{-7} to $< 1 \times 10^{-9}$ Torr in a few seconds. In the resulting UHV environment, the positron lifetime can be hours, depending upon the nature of the remaining impurities in the system. In this vacuum environment, the two-body interaction of positrons with test gases can be isolated and studied without contamination of the data due to interactions with the buffer gas molecules. As described in the next section, this ability to achieve rapid pump-down of the accumulator will be useful, for example, to shuttle positrons into a separate UHV storage and experimentation trap through a pulsed valve.

2.2. Plan for a UHV low-temperature storage trap

The buffer-gas trap is attractive for a range of applications because of the high trapping efficiency. However, many of these applications require an ultra-high vacuum (UHV) environment, and one limitation of the buffer-gas technique is that the positrons are initially in a background of nitrogen gas at a pressure $\sim 3 \times 10^{-7}$ Torr, where the annihilation time is ~ 60 s. As shown in Fig. 3, we can create a good vacuum in the trap rapidly by pumping out the buffer gas (e.g., in less than a minute). However, this interrupts the filling cycle. Thus, it is advantageous to combine rapid pump down of the accumulator with the ability to stack positron plasmas efficiently in an UHV environment. For this purpose, we are building an isolated

UHV stage, into which the positrons from the accumulator can be shuttled repetitively through a fast pulsed valve. In this way, we can isolate the efficient buffer-gas trapping from the UHV stage.

During positron accumulation, the UHV storage stage will be isolated from the positron trap by a fast valve. Then the buffer-gas feed will be switched-off, and the trap will be pumped nearly to base pressure (i.e., $\sim 1 \times 10^{-10}$ Torr in less than a minute). The gate valve will then be opened for the brief time (≤ 1 s) required to transfer the positrons to the storage trap, and the cycle will be repeated. Long confinement times and low plasma temperatures will be facilitated by applying a magnetic field of 5 T in the storage trap. In the 5 T field, the cyclotron radiation time is ~ 0.2 s. We plan to cool the walls to 4 K, and so the plasma will cool radiatively to approximately the wall temperature. The cold walls should provide excellent vacuum (e.g., pressures much less than 10^{-11} Torr). The trap will have a ‘rotating wall’ electrode for control of plasma density and increased confinement [24]. Using this device, we are likely to be able to achieve an ‘infinite’ confinement time, as has been done in the case of electron plasmas. In Table 1, the operation of the old positron accumulator is compared with that expected for the new accumulator and UHV storage stage. We assume a 6 min trapping cycle including 1 min to pump out the buffer gas and a positron loading rate of 3×10^8

Table 1
The operation of the new accumulator and the planned UHV storage stage are compared with that of the old positron accumulator^a

Parameter	Old trap	New trap and UHV stage
Source strength (mCi)	70	95
Positrons per cycle	2×10^8	$\sim 3 \times 10^8$
Cycles per hour	n.a.	10
Positrons per hour	n.a.	$\sim 3 \times 10^9$
Density (cm^{-3})	$\sim 2 \times 10^6$ ^b	$> 1 \times 10^{10}$ ^c
Base pressure (Torr)	3×10^{-10}	$< 1 \times 10^{-11}$ (cold)

^aBased on *current* new-trap performance

^bOne cycle in a 0.1 T field.

^cOne hour accumulation in a 5 T field.

per cycle which corresponds to a rate of 3×10^9 positrons per hour.

This new storage trap should be useful for a number of experiments. It effectively decouples the efficient buffer-gas accumulation process from the reservoir of cold positrons, which can then be tapped as required in an optimum manner, as needed for the particular experiment at hand. One potential application of this trap will be the production of low-energy antihydrogen [25], where high-density positron plasmas are required. Another application, positron ionization for mass-spectroscopy, can exploit the fact that the positrons in the storage trap are in a magnetic field large enough to confine large-mass ions. Thus, the interaction time of the positrons and molecules can be made long, with no loss of the ions produced.

2.3. Techniques for studying positron interactions with atoms and molecules

We briefly summarize the techniques for studying the interaction of positrons with atoms and molecules at low energies that are made available by this positron accumulator technology.

Annihilation rates. Positron annihilation rates are measured by allowing the positrons to interact with the test gas, at a given gas pressure for a fixed time, and then measuring the number of positrons remaining by dumping them on a collector or annihilation plate. This rate is found to be a linear function of test gas pressure, and the slope gives Z_{eff} . These experiments can typically be done either with the N_2 buffer gas present or absent.

Gamma-ray spectra. A high-purity Ge detector is used to measure the spectra of the annihilation gamma-ray radiation in a stage of the accumulator positioned in close proximity to the detector. Good statistics on test molecules can be obtained in a few hours or less because of the long positron-confinement times in the accumulator. The width of the gamma-ray line gives information about the quantum state (e.g., the particular molecular orbital) of the annihilating electron. In particular, the width is dominated by the momentum distribution of the valence electrons in the atom or molecule. Examples of gamma-ray spectra from H_2 and Ne are shown in Fig. 4.

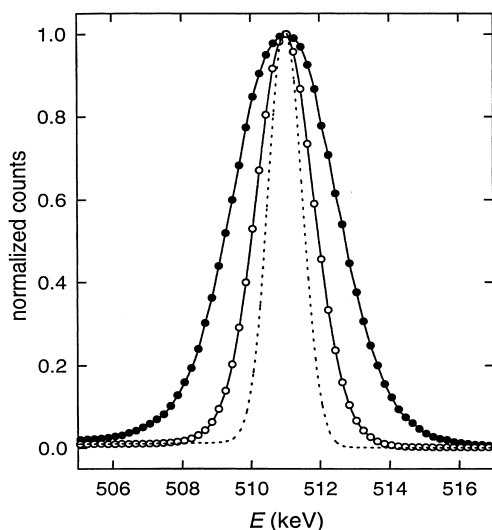


Fig. 4. Observed gamma-ray annihilation spectra from H_2 molecules (\circ) and Ne atoms (\bullet). Solid lines are drawn as a guide to the eye. The spectra are normalized to unity at the peak. The dotted line indicates the detector resolution (see [9]).

Varying positron temperature. We have developed the ability to heat the trapped positrons in order to study the dependence of the annihilation process on positron energy. This is done by applying a low-level of broad-band radio-frequency noise to one of the electrodes. Positron temperature is measured as a function of time by lowering the trapping potential and measuring the escaping tail of the positron distribution [17]. This technique is applicable for positron energies up to about 0.5 eV for atoms (e.g., noble gases) and up to a few tenths of an eV for molecules. For higher energies, it is difficult to heat the positrons and maintain a Maxwellian distribution. In molecular gases, it is likely that the dominant positron energy-loss mechanism is the excitation of high-frequency vibrational modes and this limits the thermalized positron distribution to energies ≤ 0.2 eV.

Cold positron beam. While sources of cold electron beams are common, this is not true for positrons. Recently, we developed a method to create a state-of-the-art cold positron beam using trapped positron plasmas in the accumulator [11,26,27]. The beam energy can be tuned over a very wide range from ~ 0.1 eV upwards. The

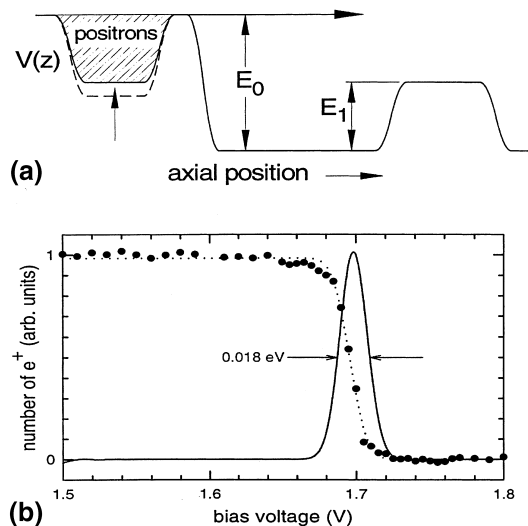


Fig. 5. (a) schematic diagram of the arrangement used to create a cold positron beam, and (b) the retarding-potential curve and energy distribution (see [26,27]).

experimental arrangement is illustrated in Fig. 5(a). Positrons are accumulated and cooled in a Penning–Malmberg trap. Then the potential of the bottom of the trap is raised, forcing the particles over a fixed-height potential barrier [energy E_0 in Fig. 5(a)], and this sets the energy of the beam. The spread in parallel energies of the beam can be as low as (or actually somewhat lower than) the temperature of the plasma in the potential well. Shown in Fig. 5(b) are data for the energy resolution of a positron beam created using this technique. We have been able to operate the beam in both continuous and pulsed modes, with the latter accomplished by reducing the depth of the confining potential well in small steps rather than continuously.

In a paper elsewhere in this volume [18], we describe progress on two topics that could not be addressed previous to the development of this beam, due to the lack of a suitable low-energy positron source. In particular, we have been able to study the excitation of molecular vibrations by positrons and also to measure the low-energy differential elastic scattering cross-sections [11]. Also discussed elsewhere are plans to use the cold beam and scattering geometry to address other topics

[11,18]. For example, we hope to be able to study elastic scattering in the regime where $ka \sim 1$, where k is the momentum of the positron and a is the s -wave scattering length (both in atomic units). In this limit, both the sign and magnitude of the scattering length, a , can be measured, and these quantities provide important information about positron–atom and positron–molecule bound states.

We believe that the limits of energy resolution of the cold positron beam have yet to be reached, even with the present apparatus. An exciting possibility would be to form the beam in the low-temperature UHV storage trap discussed in Section 2.2. In this case, it should be possible to form beams with energy spreads comparable to the cryogenic positron temperature (e.g., ~ 4 K, which corresponds to <1 meV).

3. Positron annihilation in atoms and molecules at low energies

We present here an overview of experimental studies of the annihilation of low-energy positrons on atoms and molecules, with emphasis on the large values of Z_{eff} that are observed in large molecules. We also discuss briefly theory and calculations to understand this effect. Many of the experiments are discussed in more detail in a recent paper by Iwata et al. [10].

3.1. Z_{eff} for atoms and molecules

Murphy and Surko discovered an empirical scaling relation between the logarithm of Z_{eff} and the quantity $(E_i - E_{\text{Ps}})$, where E_i is the ionization energy of the atom or molecule and E_{Ps} is the binding energy of a positronium atom [21]. This scaling is valid for all the atoms and single-bonded nonpolar molecules. In particular,

$$\ln(Z_{\text{eff}}) = A(E_i - E_{\text{Ps}})^{-1}, \quad (2)$$

where A is a positive constant. This scaling is illustrated in Fig. 6. There is no apparent distinction between atoms and molecules. This scaling was

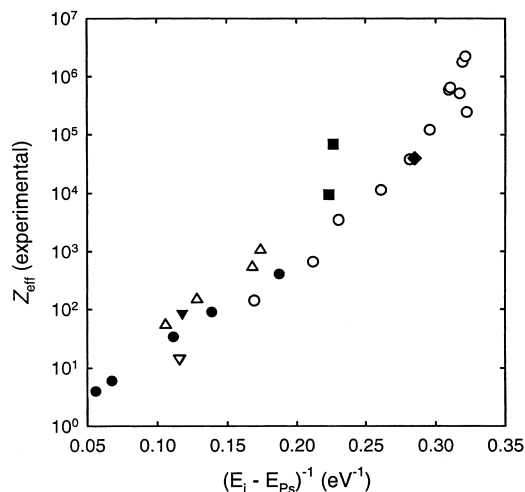


Fig. 6. Scaling of Z_{eff} with $(E_i - E_{\text{Ps}})^{-1}$: (●) noble gases, (▽) H_2 , (▼) SF_6 , (○) alkanes, (△) perfluorinated alkanes, (■) perchlorinated alkanes, and (◆) CBr_4 (see [21]).

found not to be a good predictor of Z_{eff} for polar molecules or ones with double bonds. The peak-to-peak spread in measured Z_{eff} values is generally better than one order of magnitude. To the extent that this simple relation matches the data, this scaling indicates that it is the electronic structure of the molecule that determines the annihilation rate. In this picture, other aspects of molecular structure, such as the character of the vibrational modes, appear to play a relatively minor role in determining the annihilation rate.

3.2. Identification of annihilation sites from the gamma-ray spectra

As discussed above, the annihilation gamma-ray spectrum contains information about the momentum distribution of the electrons participating in the annihilation process. In a precision experiment in helium, we were able to test a state-of-the-art theoretical calculation of positrons interacting with this atom, by measuring the gamma-ray annihilation lineshape [28]. These results were compared with calculations by Van Reeth and Humberston, using the Kohn variational approximation and very accurate wave functions [28]. Theory and experiment are in agreement over

three orders of magnitude in spectral amplitude. The challenge is to extend this level of understanding to larger atoms and molecules.

We have made annihilation rate and gamma-ray spectral measurements for a wide range of molecules [4,8,9]. A particularly significant experiment was the study of annihilation sites in alkanes and partially fluorinated hydrocarbon molecules. Fig. 7(a) shows the observed line widths of the gamma-ray spectra for alkanes plotted against the fraction of valence electrons in C–C bonds. The momentum distributions of electrons in the C–H and C–C bonds of hydrocarbons have been calculated and found to be distinctly different [29]. The linear relationship observed in Fig. 7(a) leads us to conclude that positrons annihilate with equal probability on any valence electron in the alkane molecules. Similarly, we have found that the measured gamma-ray spectra from partially fluorinated hydrocarbons can be fit accurately using a linear combination of the experimentally measured (analogous) hydrocarbon and perfluorinated carbon spectra (e.g., by fitting the C_2H_5F spectrum with the measured C_2H_6 and C_2F_6 spectra) [9]. These fits yield the fraction of annihilations on fluorine atoms. The resulting values are plotted against the fraction of valence electrons on fluorine atoms in Fig. 7(b). As in the case of the alkanes, the linear relationship indicates that positrons annihilate with equal probability with

any of the valence electrons in the fluorinated and partially fluorinated hydrocarbon molecules. Thus, it appears to be a general result that low-energy positrons annihilate with approximately equal probability on any valence electron. This can be interpreted to mean that the positron has a relatively long de Broglie wavelength in the vicinity of the molecule and consequently interacts with roughly equal probability with any of the valence electrons. This is in contrast to the case where the positron is localized at a specific molecular site, as would be expected in a tight-binding model.

The conclusion reached from these experiments is in agreement with the calculations of Crawford [30], who considered the fragmentation of molecules following positron annihilation. He found that most valence molecular orbitals produce comparable annihilation probabilities, and since the highest lying molecular orbital does not dominate the annihilation process, the molecule is typically left in an excited electronic state. In Crawford's theory, these excited states lead to the extensive fragmentation that is observed in experiment at low values of incident positron energy.

The positron-nuclear potential is repulsive, and so the low-energy positrons do not penetrate appreciably into the electron cloud. Thus, it is not surprising that annihilation occurs predominantly on the valence electrons [9]. However, a small

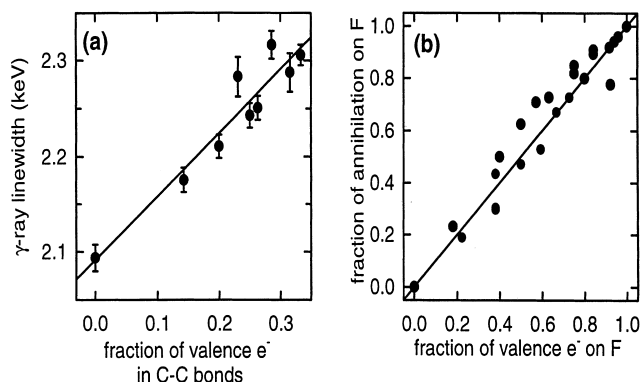


Fig. 7. (a) Gamma-ray line width (\bullet) for alkanes, plotted against the fraction of valence electrons in C–C bonds, and (–) a fit to the data. (b) Fraction of annihilation on fluorine atoms (\bullet) for partially fluorinated hydrocarbons, plotted against the fraction of valence electrons on these atoms, and (–) the line $y = x$. These linear relationships provides evidence that positrons annihilate with approximately equal probability on any valence electron (see [9]).

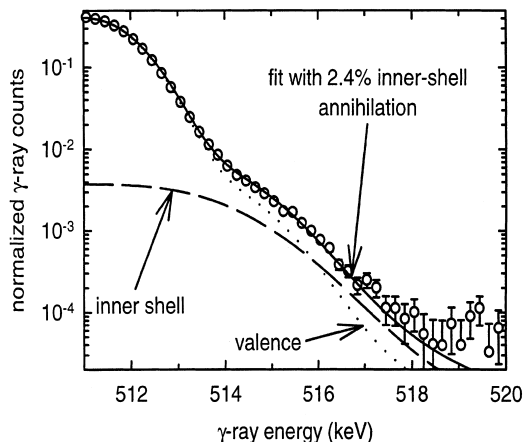


Fig. 8. Positron annihilation gamma-ray spectrum from Xe: (○) Experimental data, (—) fit using a theoretically calculated spectra with 2.4% inner-shell component; (·····) the corresponding valence electron and (---) inner-shell electron component (see [32]).

fraction of positrons can tunnel through the repulsive potential and annihilate with inner-shell electrons, and this leads to much broader components in the spectra [31]. We are now able to study this effect experimentally [32]. As an example, the gamma-ray spectrum for Xe is shown in Fig. 8. The annihilation gamma-ray spectrum from each subshell was calculated using the static Hartree–Fock approximation [32]. We found that we are able to fit the observed spectrum by adjusting the amplitude of the calculated inner-shell spectrum relative to that of the valence electron component. This fit indicates that 2.4% of the positrons annihilate with inner-shell electrons in Xe. Similar studies of other noble gases indicate 1.3% inner-shell annihilation in Kr and less than 0.2% in Ar. Based on these results, we expect that inner-shell annihilation should generally occur at the few percent level in heavier atoms, and is likely to be much less frequent (e.g., $\leq 0.1\%$ of the annihilations) in light atoms, such as carbon.

3.3. Dependence of annihilation rates on positron temperature

Using the technique described above to heat the positrons in the accumulator, we have been able to

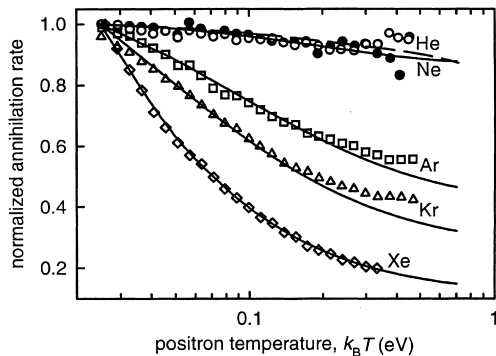


Fig. 9. Temperature dependence of positron annihilation rates on noble gases. Experimental data: (●) He, (○) Ne, (□) Ar, (△) Kr, and (◇) Xe. Also shown are theoretical calculations, using the Kohn variational approximation for He (—) [28] and the polarized orbital approximation for the other atoms (---) [33–35] (see [17]).

study the dependence of annihilation rates on positron temperature for noble gas atoms [17]. The measured values of Z_{eff} are plotted in Fig. 9, where the data are normalized to their room-temperature values. The theoretically calculated temperature dependences, based on the polarized orbital approximation, are shown for Ne, Ar, Kr and Xe [33–35], and the calculation described in Section 3.2 for He [28], are also shown in the figure. While these predictions for the dependence of Z_{eff} on temperature are in excellent agreement with experiment, we note that the predicted and measured absolute values of Z_{eff} (for noble gases heavier than He) do not agree well [8,35,36].

We have also made the first studies of the positron-temperature dependence of annihilation rates for *molecules* [10]. These experiments have the potential to shed light on a number of issues, such as the role of molecular vibrations in the anomalously large annihilation rates observed for large molecules. Shown in Fig. 10 are data for three alkane and deuterated alkane molecules. The data show approximately universal behavior for these molecules. In contrast, these molecules have very different absolute values of Z_{eff} , ranging from methane with $Z_{\text{eff}} \sim 150$ to butane with $Z_{\text{eff}} \sim 10^4$. The plateau at higher positron temperatures may be due to the excitation of molecular vibrations. As discussed below, we expect to be able to

address a number of important questions with extensions of these kinds of measurements to higher positron energies using the cold positron beam. For example, as shown in Fig. 11, fluori-

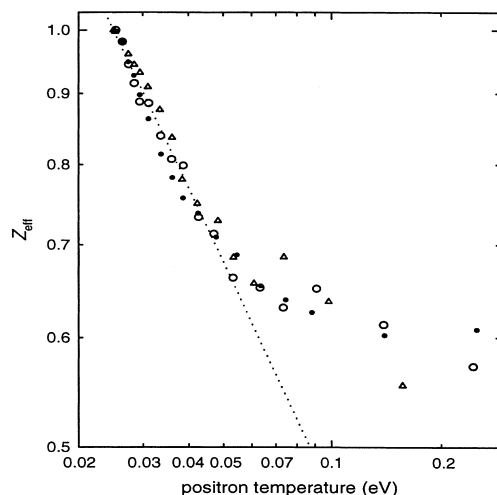


Fig. 10. Temperature dependence of the annihilation rates for methane (○), deuterated methane (△), and butane (●). The dotted line (···) is a power-law fit to the data at low temperatures, yielding a coefficient of -0.55 (see [10]).

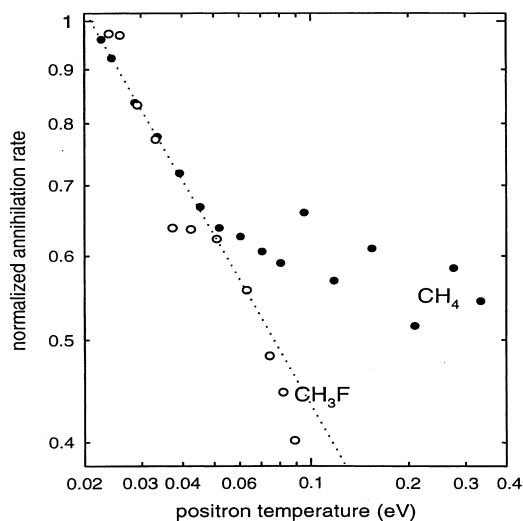


Fig. 11. Dependence of annihilation rates on positron temperature: (●) methane (CH_4), and (○) fluoromethane (CH_3F). The annihilation rates are normalized to their room-temperature values. The dotted line (···) is an exponential fit to the lower temperature data with an exponent of -0.53 (see [10]).

nated hydrocarbons exhibit a different behavior at the higher positron energies than that observed for the alkanes. It will also be interesting to study this effect in chemical species, such as chlorocarbons and bromocarbons.

A large-scale computer calculation has been carried out recently for low-energy positrons interacting with ethylene (C_2H_4) [20]. The results for Z_{eff} and its temperature dependence, which are plotted in Fig. 12, agree well with our measurements [10]. We note that this calculation does not take into account the vibrational motion of the atoms. Thus the relatively large value of Z_{eff} that is predicted is due to the nature of the *electronic* states (i.e., not the vibrational states) in the molecule.

The data at smaller values of positron energy in both Figs. 10 and 11 can be fit to a power law of the form $Z_{\text{eff}} \sim T^{-\eta}$, with $\eta \cong 0.5$. The possible significance of this scaling is discussed in the papers by Iwata et al. [10] and Gribakin [19].

3.4. Other experiments

The question has arisen as to the possible role that vibrational excitations play in the large Z_{eff} values that are observed in large molecules. To test this, the annihilation rates of deuterated and protonated alkanes were measured systematically, and the results are shown in Fig. 13 [10]. The

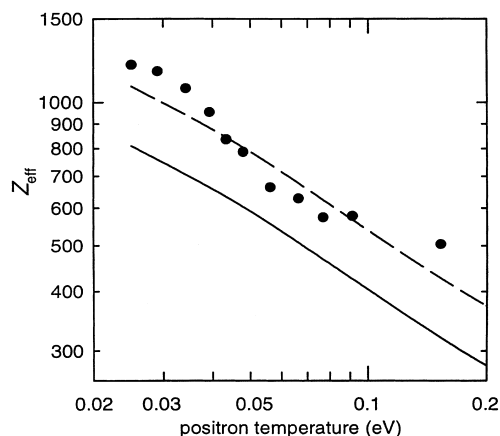


Fig. 12. Temperature dependence of the annihilation rate for ethylene; experiment (●) and calculation (—) [20]. The dashed line (---) is the calculation scaled by a factor of 1.3 (see [10]).

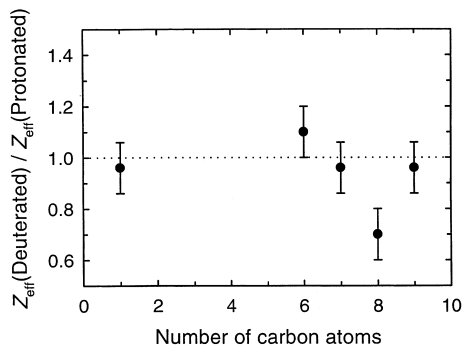


Fig. 13. The ratios of Z_{eff} for deuterated alkanes to those for protonated alkanes, plotted as a function of the number of carbon atoms, j (see [10]).

annihilation rates for the deuterated and protonated alkanes are very similar if not identical. While a factor of 2–3 change in annihilation rate was observed previously for deuterated benzenes [8], the systematic study of alkanes presented here does not provide support for a mechanism in which the positron forms long-lived vibrationally excited resonant states with molecules. This negative result would be natural if the annihilation process involved only electron–positron degrees of freedom. Another possibility is that only low-frequency vibrational modes are involved in the formation of positron–molecule resonances (i.e., the low frequency modes in alkane molecules would not be changed significantly by deuteration).

Systematic study of Z_{eff} in hydrocarbons as a function of fluorine substitution has also proven interesting. These experiments are described in more detail in the paper by Iwata et al. [10]. The annihilation rate is found to be nonmonotonic in the number of fluorine atoms added. It increases with the addition of one fluorine, and then decreases significantly for larger numbers of fluorines. All fully fluorinated compounds studied have much lower values of Z_{eff} than the analogous hydrocarbons. Gribakin has constructed a theory in which this effect is due to a change in the nature of the positron–molecule potential with the substitution of fluorines for hydrogen atoms [10,19]. In this picture, positrons are predicted to bind to the hydrocarbons but not to the fully fluorinated molecules. The maximum in Z_{eff} is then explained

as the positron–molecule potential for which bound level goes to zero and the scattering length diverges. We refer the reader to the papers by Iwata et al. and Gribakin for further details [10,19].

3.5. Relationship to theory

Current theory and calculations regarding positron annihilation in molecules can be found in the work of Gribakin [19] and da Silva et al. [20]. Gribakin has considered two mechanisms for annihilation. One is direct annihilation, which can be enhanced by an attractive positron–molecule interaction, including the possible presence of positron–molecule bound states. A second mechanism is resonant annihilation, which can lead to larger values of Z_{eff} if the excitation of molecular vibrations occurs in the presence of an attractive positron–molecule potential. Gribakin estimates that direct annihilation is capable of giving $Z_{\text{eff}} \leq 10^3$, while resonant annihilation, which involves positron capture into the vibrationally excited states of the positron–molecule complex, can produce values of Z_{eff} as large as 10^8 .

In the case of direct annihilation, large annihilation rates will be observed if there are weakly bound states or low-lying virtual levels. Studies of annihilation in fluorinated hydrocarbons lend support to this picture [10]. For molecules that possess a broad spectrum of vibrational resonances, Gribakin predicts that resonant annihilation will dominate. To test this model, we conducted measurements of annihilation rates of deuterated alkanes, illustrated in Fig. 13 [10]. This test did not provide support for the predictions of the simplest interpretation of the resonant annihilation model.

These two annihilation mechanisms do not involve Ps formation in a direct way. In addition, resonant annihilation directly involves the molecular vibrations. In contrast, the empirical scaling described by Eq. (2) seems to indicate that the dominant mechanism for enhanced annihilation rates involves only the electronic structure of the atom or molecule (i.e., not the molecular vibrational modes). We speculate that, if there were low-lying *electronic* excitations of a positron–atom

or molecule complex, then a resonance model such as that described above might be possible. In this case, the resonant modes would now be electronic, as opposed to vibrational, in nature. To our knowledge, there is no analogous phenomenon involving low-lying electronic excitations in electron–molecule interactions, and so the positron would have to play a fundamental role in these modes. We have speculated previously that the Murphy scaling might correspond to a physical picture of a Ps atom moving in the field of the positively charged molecular ion. Short-range correlations between the positron and electrons would be important in producing large annihilation rates. It poses a challenge to theory to include short-range correlation into the scattering problem.

Recent advances in computational approaches have enabled large-scale calculations of positron–molecule interactions to be carried out for small molecules such as ethylene. The agreement between theory and experiment for ethylene, illustrated in Fig. 12 is encouraging [20]. Vibrational motion is not included in these calculations. The large annihilation rate that is predicted and observed illustrates the importance of short-range electron–positron correlations in determining annihilation rates. If these calculations could be done for larger molecules, they would offer the possibility of testing

the theoretical prediction that vibrations are required for annihilation rates $Z_{\text{eff}} \geq 10^3$.

4. Possibilities for future experiments

We take the opportunity to describe some important open questions and experiments that are either possible now, or will be in the near future, to answer these questions. Continuing in the spirit of this paper, we highlight experiments that use the positron trapping and cold beam technologies to study positron annihilation in atoms and molecules. In the paper by Gilbert et al., elsewhere in this topical issue [18], we make similar comments about the potential of the cold positron beam to extend our knowledge of low-energy positron interactions with atoms and molecules through scattering experiments.

Annihilation studies with the cold positron beam.

Annihilation-rate measurements as a function of positron energy for a wide range of energies (i.e., $0.1 \leq E \leq E_{\text{Ps}}$, where E is the positron's energy) can be accomplished by passing the cold positron beam through a gas cell. A schematic diagram of such an experiment is shown in Fig. 14. The gamma-ray detector should be designed to optimize collection efficiency, while minimizing the background due to positron annihilation on other

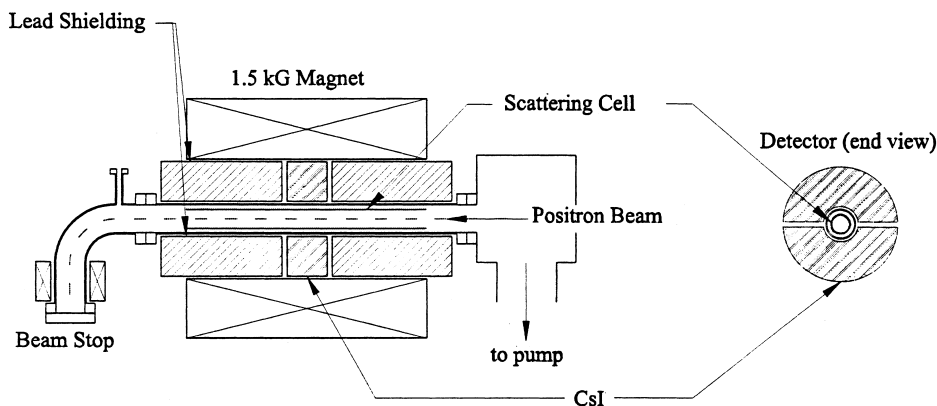


Fig. 14. Schematic diagram of apparatus proposed to measure annihilation rates as a function of positron energy using the cold beam. The energy resolution and range of positron energies that can be studied is much greater than that which can be achieved by heating the positrons in the accumulator.

than the target atoms or molecules. The signal will be proportional to the Z_{eff} of the specific atom or molecule. For example, for C_6H_{14} at a pressure of 10^{-5} Torr, $Z_{\text{eff}} = 120,000$, and we expect a count rate of $\sim 10^5$ h. For methane and helium at pressures of 10^{-3} Torr, we expect count rates of $\sim 10^4$ and 100 h^{-1} , respectively. Study of methane and larger molecules should be possible in a single pass of the positron beam. The signal to noise for smaller molecules and atoms will depend upon the magnitude of the background signal. The sensitivity of this experiment could be greatly improved if the beam makes *multiple passes in the gas cell* without too much energy loss. The acceptable number of transits, still maintaining good energy resolution, will be determined by the rate at which the positrons lose energy through inelastic scattering. This can be determined by trapping the positrons for a varying amounts of time and then measuring the energies of the trapped positrons.

Laricchia and Wilkin have raised the intriguing question as to the asymptotic form of Z_{eff} when the positron energy is increased to E_{Ps} [37,38]. There is general agreement that, below the threshold for positronium formation, Z_{eff} will diverge as a function of the parameter $\xi = E - E_i + E_{\text{Ps}}$, where E_i and E_{Ps} are defined in Eq. (2). Laricchia and Wilkin predict that $Z_{\text{eff}} \sim \xi^{-1}$, while Humberston and Van Reeth [39,40] and Dzuba et al. [36] predict $Z_{\text{eff}} \sim \xi^{-1/2}$. This can be tested using the cold positron beam and the apparatus as shown in Fig. 14.

Materials with low vapor pressures. A number of outstanding questions regarding positron annihilation in atomic and molecular species have proven difficult to study experimentally at room temperature due to the relatively low vapor pressure of the particular material. For example, as we have discussed, annihilation rates for large molecules are typically much larger than can be explained on the basis of simple collisions. The largest alkane studied to date is $\text{C}_{16}\text{H}_{34}$ [12]. It is expected that the annihilation rate per molecule will saturate as a function of molecular size for molecules moderately larger than this (i.e., when each collision leads to an annihilation, which would correspond to a positron dwell time on the molecule $\sim 10^{-10}$ s) [8].

This and other experiments discussed below would be possible if the annihilation cell containing the test gas (e.g., shown in Fig. 14) could be elevated in temperature (e.g., $T \leq 350\text{--}500$ K). However, because of the proximity of this cell to the positron accumulator, the design of such an experiment will be a challenge. Excellent vacuum isolation of the gas cell from the positron accumulator will be required, since these materials are expected to have very large annihilation rates, and so they present a serious source of contamination of the positron accumulator. Since they have low vapor pressures, they will be difficult to remove from walls of the accumulator vacuum chamber, even at elevated temperatures. We believe that both geometrical isolation (i.e., avoiding line-of-sight connection between the hot cell and the accumulator) and cold walls in the isolation stage will be necessary.

Another interesting candidate for study in an annihilation cell at elevated temperatures would be the large hydrocarbon molecule, pyrene, which is composed of an arrangement of four benzene rings. It is prototypical of polycyclic aromatic ('PAH') molecules present in the interstellar medium and is expected to have values of Z_{eff} in excess of 10^7 . The high annihilation rate of this molecule has potentially important implications in astrophysics [41]. The high-temperature annihilation cell described here would also permit study of atomic clusters, such as C_{60} .

Atomic species with low vapor pressures at room temperature will also be of interest. For example, metal atoms can provide an important test of the empirical scaling law for Z_{eff} , given by Eq. (2). This relationship holds for all atoms studied to date. If this holds true in general, then atoms such as gold, zinc and cadmium would be predicted to have Z_{eff} values larger than dodecane (i.e., $\text{C}_{12}\text{H}_{26}$, with $Z_{\text{eff}} \sim 2 \times 10^6$), and atoms such as lead, bismuth, silver and tin would have even larger annihilation rates. All theories of high annihilation rates of which we are aware require internal degrees of freedom of the target species, such as molecular vibrations. If metal atoms also have very high values of Z_{eff} , this would imply that the electronic degrees of freedom of the positron-target complex are sufficient to observe this

remarkable effect (i.e., as mentioned above), which would be contrary to conventional wisdom.

Auger electrons. The measurements of annihilation on inner shell electrons in noble gas atoms provide quantitative predictions for the frequency at which Auger electrons will be produced in the annihilation process. We should be able to test this experimentally by measuring directly the production rate of these Auger electrons.

Positron ionization and fragmentation. The ionization of molecules by positron annihilation was first studied by Passner et al. [42]. Later, Hewlett and co-workers studied many aspects of this effect in detail [43]. One very interesting phenomenon is their discovery that, at the threshold for positronium formation, the ions do not fragment, while both below and above this energy, there is extensive fragmentation. Many open questions remain regarding this phenomenon. It is a potentially important means to ionize large molecules for mass spectroscopic analysis, where varying and controlling fragmentation is an important issue. With the cold positron beam, one could study with greater precision the phenomenon of reducing fragmentation when the positron's energy is tuned to the threshold for positronium formation. The high-field trap described in Section 2.2 offers the potential to confine the heavy-ion fragments produced by annihilation, thereby exploiting the long positron confinement time available with a positron trap to maximize the positron-molecule interaction, but without losing the ions produced via annihilation.

5. Summary

This paper presents an overview of the ongoing development of accumulator-based technology for manipulating positron plasmas, and the use of this technology to study the interaction of low energy positrons with atoms and molecules. There has been much progress in this area. Relatively compact, robust and less expensive positron accumulators are now available that can furnish positrons efficiently to a UHV environment for experiment. Accumulator-based, cold positron beams are in their infancy, but they have now begun to be used

in atomic physics experiments. These technological advances enable a broad range of experiments to study the interaction of low-energy positrons with atoms and molecules.

Many interesting topics remain to be addressed in this area. The cold beam will enable the study of the vibrational excitation of molecules by positrons and careful searches for resonances in atomic cross sections. It also offers the opportunity to study differential elastic scattering cross sections at low energies (e.g., less than 1 eV). New tools are available to study annihilation in large molecules to understand the origin of the large annihilation rates that have been observed. A natural extension of this work would be to study annihilation in atomic clusters and dust grains. This would make the connection between the atomic and molecular physics, which is the focus of this paper, and condensed matter physics and astrophysics. The experimental advances described here, coupled with recent progress in the theory of positron-atom and positron-molecule interactions, bode for an interesting future for science in this area.

Acknowledgements

This work is supported by the National Science Foundation, Grant No. PHY 96-00407 and the Office of Naval Research under Grant No. N00014-96-10579. We wish to thank Gleb Gribakin for insightful discussions regarding theoretical aspects of positron interactions with atoms and molecules. We thank Gene Jerzewski for his expert technical assistance and James Sullivan for help with a number of aspects of this manuscript.

References

- [1] D.M. Schrader, R.E. Svetic, *Can. J. Phys.* 60 (1982) 517.
- [2] W.E. Kauppila, T.S. Stein, *J. Adv. Atomic, Mol. and Opt. Phys.* 26 (1990) 1.
- [3] M. Charlton, G. Laricchia, *J. Phys. B* 23 (1990) 1045.
- [4] S. Tang, M.D. Tinkle, R.G. Greaves, C.M. Surko, *Phys. Rev. Lett.* 68 (1992) 3793.
- [5] O. Sueoka, A. Hamada, *J. Phys. Soc. Jpn* 62 (1993) 2669.
- [6] R.J. Drachman, *The Phys. of Elec. and At. Coll.*, AIP Conf. Proc., AIP, New York, 1995, p. 389.

- [7] J. Xu, J.L.D. Hulett, T.A. Lewis, S.A. McLuckly, *Phys. Rev. A* 52 (1995) 2088.
- [8] K. Iwata, R.G. Greaves, T.J. Murphy, M.D. Tinkle, C.M. Surko, *Phys. Rev. A* 51 (1995) 473.
- [9] K. Iwata, R.G. Greaves, C.M. Surko, *Phys. Rev. A* 55 (1997) 3586.
- [10] K. Iwata, G. Gribakin, R.G. Greaves, C. Kurz, C.M. Surko, *Phys. Rev. A* 61 (2000) 022719.
- [11] S.J. Gilbert, R.G. Greaves, C.M. Surko, *Phys. Rev. Lett.* 82 (1999) 5032.
- [12] C.M. Surko, A. Passner, M. Leventhal, F.J. Wysocki, *Phys. Rev. Lett.* 61 (1988) 1831.
- [13] T.J. Murphy, C.M. Surko, *Phys. Rev. A* 46 (1992) 5696.
- [14] R.G. Greaves, C.M. Surko, *Phys. Plasmas* 4 (1997) 1528.
- [15] D.A.L. Paul, L. Saint-Pierre, *Phys. Rev. Lett.* 11 (1963) 493.
- [16] G.R. Heyland, M. Charlton, T.C. Griffith, G.L. Wright, *Can. J. Phys.* 60 (1982) 503.
- [17] C. Kurz, R.G. Greaves, C.M. Surko, *Phys. Rev. Lett.* 77 (1996) 2929.
- [18] S. Gilbert, J. Sullivan, R.G. Greaves, C.M. Surko, *Nucl. Instr. and Meth. B* 171 (2000) 81.
- [19] G. Gribakin, *Phys. Rev. A* 61 (2000) 022720.
- [20] E.P. da Silva, J.S.E. Germane, M.A.P. Lima, *Phys. Rev. Lett.* 77 (1996) 1028.
- [21] T.J. Murphy, C.M. Surko, *Phys. Rev. Lett.* 67 (1991) 2954.
- [22] J.H. Malmberg, C.F. Driscoll, *Phys. Rev. Lett.* 44 (1980) 654.
- [23] T.J. Bartel et al., *Icarus: A 2D Direct Simulation Monte Carlo (DSMC) Code for Parallel Computers*, Users Manual-V3.0, Sandia National Laboratories Report SAND96-0591, 1996.
- [24] F. Andereg, E.M. Hollmann, C.F. Driscoll, *Phys. Rev. Lett.* 81 (1998) 4875.
- [25] C.M. Surko, R.G. Greaves, M. Charlton, *Hyperfine Interactions* 109 (1997) 181.
- [26] S.J. Gilbert, C. Kurz, R.G. Greaves, C.M. Surko, *Appl. Phys. Lett.* 70 (1997) 1944.
- [27] C. Kurz, S.J. Gilbert, R.G. Greaves, C.M. Surko, *Nucl. Instr. and Meth. B* 143 (1998) 188.
- [28] P. Van Reeth, J.W. Humberston, K. Iwata, R.G. Greaves, C.M. Surko, *J. Phys. B* 29 (1996) L465.
- [29] S.Y. Chuang, B.G. Hogg, *Can. J. Phys.* 45 (1967) 3895.
- [30] O.H. Crawford, *Phys. Rev. A* 49 (1994) R3147.
- [31] K.G. Lynn, A.N. Golland, *Solid State Commun.* 18 (1976) 1549.
- [32] K. Iwata, G. Gribakin, R.G. Greaves, C.M. Surko, *Phys. Rev. Lett.* 79 (1997).
- [33] R.P. McEachran, A.G. Ryman, A.D. Stauffer, *J. Phys. B* 11 (1978) 551.
- [34] R.P. McEachran, A.G. Ryman, A.D. Stauffer, *J. Phys. B* 12 (1979) 1031.
- [35] R.P. McEachran, A.D. Stauffer, L.E.M. Campbell, *J. Phys. B* 13 (1980) 1281.
- [36] V.A. Dzuba, V.V. Flambaum, G.F. Gribakin, W.A. King, *Phys. B* 29 (1996) 3151.
- [37] G. Laricchia, C. Wilkin, *Phys. Rev. Lett.* 79 (1997) 2241.
- [38] G. Laricchia, C. Wilkin, *Nucl. Instr. and Meth. B* 143 (1998) 135.
- [39] P. Van Reeth, J.W. Humberston, *J. Phys. B* 31 (1998) L231.
- [40] J.W. Humberston, P. Van Reeth, *Nucl. Instr. and Meth. B* 143 (1998) 127.
- [41] K. Iwata, R.G. Greaves, C.M. Surko, *Canadian J. Phys.* 51 (1996) 407.
- [42] A. Passner, C.M. Surko, M. Leventhal, A.P. Mills Jr., *Phys. Rev. A* 39 (1989) 3706.
- [43] L.D. Hulett Jr., D.L. Donohue, J. Xu, T.A. Lewis, S.A. McLuckey, G.L. Glish, *Chem. Phys. Lett.* 216 (1993) 236.